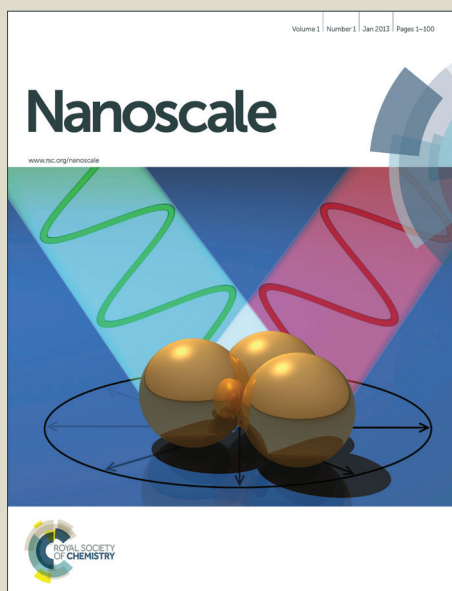


Nanoscale

Accepted Manuscript



This is an *Accepted Manuscript*, which has been through the Royal Society of Chemistry peer review process and has been accepted for publication.

Accepted Manuscripts are published online shortly after acceptance, before technical editing, formatting and proof reading. Using this free service, authors can make their results available to the community, in citable form, before we publish the edited article. We will replace this *Accepted Manuscript* with the edited and formatted *Advance Article* as soon as it is available.

You can find more information about *Accepted Manuscripts* in the [Information for Authors](#).

Please note that technical editing may introduce minor changes to the text and/or graphics, which may alter content. The journal's standard [Terms & Conditions](#) and the [Ethical guidelines](#) still apply. In no event shall the Royal Society of Chemistry be held responsible for any errors or omissions in this *Accepted Manuscript* or any consequences arising from the use of any information it contains.

Efficient optical-electrochemical dual probe for highly sensitive recognition of dopamine based on terbium complexes functionalized reduced graphene oxide

Zhan Zhou ^b, Qianming Wang ^{a,b,c*}

^a *Key Laboratory of Theoretical Chemistry of Environment, Ministry of Education, School of Chemistry and Environment, South China Normal University, Guangzhou 510006, P. R. China*

^b *School of Chemistry and Environment, South China Normal University, Guangzhou 510006, P. R. China*

^c *Guangzhou Key Laboratory of Materials for Energy Conversion and Storage 510006, P. R. China*

* To whom the correspondence should be addressed. E-mail: qmwang@scnu.edu.cn
Tel: 86-20-39310258; Fax: 86-20-39310187

Abstract

A novel organic-inorganic hybrid sensor based on diethylenetriaminepentaacetic acid (DTPA) modified reduced graphene oxide (RGO-DTPA) chelated with terbium ions allows detection of dopamine (DA) through an emission enhancement effect. Its luminescence, peaking at 545 nm, has been improved by a factor of 25 in the presence of DA (detection limit = 80 nM). In addition, this covalently bonded terbium complexes functionalized reduced graphene oxide (RGO-DTPA-Tb) can be successfully assembled on a glassy carbon electrode. The assay performed through differential pulse voltammetry (DPV) yielded obvious peak separation between DA and excessive amounts of the interfering ascorbic acid (AA).

Keywords: Graphene oxide, Terbium, Luminescence, Electrochemical

Introduction

Dopamine (DA), a catecholamine neurotransmitter, is widely distributed in mammalian central nervous systems.^{1,2} Abnormal levels of DA in human body are associated with various diseases such as Schizophrenia and Parkinson's disease.^{3, 4} Therefore, methods for quantitative detection of DA such as high-performance liquid chromatography (HPLC),⁵⁻⁷ capillary electrophoresis,^{8, 9} fluorimetry,¹⁰⁻¹³ and electrochemical analysis,¹⁴⁻¹⁸ have been developed. Although electrochemistry has attracted wide attention due to its convenience, high sensitivity and reproducibility, a major problem is the interference by ascorbic acid (AA), which has oxidation potential close to that of DA at conventional electrodes. Therefore, it is imperative to develop a simple, sensitive, selective and reliable analytical technology for the determination of DA in the presence of AA.

Graphene and its derivatives, such as graphene oxide (GO) and reduced graphene oxide (RGO), have unique mechanical, thermal and electrochemical properties.¹⁹ Meanwhile, owing to their special physical and chemical properties, graphene and its derivatives have been incorporated into numerous functional materials to form composites through chemical and functionalizations.²⁰⁻²⁵ These graphene-based functional materials have been used for Raman enhancement, in photovoltaic devices, in photocatalysis, and in sensing platforms.²⁶⁻³⁰

Lanthanide-based luminescent materials have received much attention due to their sharp emission bands, large Stokes shifts and a wide range of lifetimes, and have been used as optical probes in bioimaging and sensing of biological analytes.³¹⁻³⁷ Here we describe a terbium complex bonded to a graphene platform and demonstrate its utility in both fluorescent and electrochemical detection of DA with high sensitivity and selectivity. Diethylenetriamine

pentaacetic acid dianhydride (DTPAda) was employed to react GO to form DTPA-modified reduced GO with surface carboxyl groups that can coordinated with terbium ions (see the synthetic process in Fig. S1). Luminescence of the material (RGO-DTPA-Tb) was enhanced in the presence of DA but not for other interfering substances (including AA). When assembled onto the surface of a glassy carbon electrode (GCE), RGO-DTPA-Tb served as a working electrode. Differential-pulse voltammetry (DPV) measurements are carried out and it has been found that only dopamine could give rise to peak current changes during the redox processes. To the best of our knowledge, this is the first time that the reduced graphene oxide based lanthanide hybrid optical switch has been fabricated and its electrochemical responses to DA has never been reported.

Results and discussion

The XRD patterns of natural graphite, GO and RGO-DTPA are shown in Fig. S2. In the curve obtained from the natural graphite sample, a sharp and intense peak located at 26.6° (d -spacing = 0.34 nm) corresponds to the 002 reflection. However, the feature reflection peak appears at 10.9° (corresponding to a d -spacing of 0.78 nm) for GO, indicating that the d -spacing increased due to the intercalation of oxygen functionalities between layers of the graphite.³⁸ After reduction and modification of the GO surface with DTPA, the peak at 10.6° disappeared. In the RGO-DTPA sample, a very weak and broad diffraction peak was observed at 24° , indicating that GO was reduced by the DTPA derivative and that the alkyl chains do not prevent re-aggregation of graphene completely when they are dried.

The FT-IR spectra of GO were characterized by three peaks at 3169, 1722 and 1624 cm^{-1}

corresponding to O-H, C=O and C=C stretching vibrations, respectively (Fig. S3a). After modification with 1,4-butanediamine, three adjacent peaks at 2928, 2866 and 2808 cm^{-1} due to stretching vibrations of the CH_2 moieties of the alkyl chain were observed. Moreover, the -COOH stretching vibration (located at 1722 cm^{-1}) disappeared in the IR spectra of RGO-NH₂ (Fig. S3b) indicating that GO was completely reduced by 1,4-butanediamine. However, in the RGO-DTPA curve (Fig. S3c), the peak at 1708 cm^{-1} (ν_{COOH}) was again observed, proving that DTPA was covalently grafted onto the graphene sheets. The intensity of the ν_{COOH} peak in the IR spectrum of RGO-DTPA (Fig. S3c) was higher than that in the RGO-DTPA-Tb curve (Fig. S3d), indicating that the coordination with the terbium ions led to this signal change.

We studied the morphology of pure GO and RGO-DTPA-Tb by TEM, HR-TEM, SAED and SEM. The large sheets of GO are situated on the top of the carbon-coated Cu-grid, resembling silk veil waves (Fig. S4). The SAED pattern of GO (Fig. S4, inset) has diffraction rings and the diffraction dots are unresolved, which may support an amorphous nature of GO. Compared with the TEM image of GO, RGO-DTPA-Tb (Fig. 2a) displays a lamellar morphology and curled edges. These are not observed prior to modification with the terbium complexes. In the HR-TEM images of RGO-DTPA-Tb (Fig. 2b), we can clearly see a number of layers in the edge of graphene. SAED analysis of this region (Fig. 2b, inset) reveals well-defined diffraction spots that confirm the crystalline structures of RGO-DTPA-Tb. It has been found that the functional organic groups can be successfully attached on the surface of graphene.³⁹ Similar structures and graphene wrinkles were also obtained in SEM images of RGO-DTPA-Tb (Fig. S5).

The dopamine sensing abilities of RGO-DTPA-Tb were investigated in fluorescence

titrations experiments. Fig. 3 is a plot of the luminescence response of the probe upon DA introduction into the aqueous system (excited at 300 nm). As seen from the spectra, the emission peak (at 545 nm) of the probe prior to DA addition was very weak due to the absence of chromophore in the ligand (DTPA derivative). Addition of small aliquots of DA solution enhanced the emission intensities of the RGO-DTPA-Tb in terms of efficient energy transfer from the DA ligands to the terbium ions. Narrow-width emission bands with maxima at 490, 545, 585, and 622 nm were assigned to the characteristic transitions of the Tb³⁺ ions, from ⁵D₄ energy level to ⁷F_J multiplets (*J* = 6, 5, 4, and 3), respectively. The emission intensity at 545 nm was correlated with DA concentration from 0.5 to 10 μM. In this case, a color change was detected by unaided eyes upon UV excitation, even at a DA concentration of 10 μM (Fig. 1, inset photo). The emission intensity change (545 nm) *versus* the concentration of DA follow the simple linear equation $y = 21.93 + 118.3x$ ($R^2=0.9957$), and a detection of limit (80 nM) was calculated using the equation $DL = 3 \times SD$ (standard deviation) / slope (Fig. 3 inset).⁴⁰ The luminescence intensities at the tested DA concentrations are summarized in Table S1. Moreover, the RGO-DTPA-Tb sensor shows quick response time (5-10 s) upon adding DA to the sensor solution, thus enabling a rapid detection of DA.

Selectivity is a critical parameter to evaluate the performance of a fluorescent sensor. Possible interference with DA detection from potentially coexisting compounds (AA, glucose, lactose, citrate, lysine, arginine, tryptophan, methionine, alanine) and ions (K⁺, Ca²⁺, Mg²⁺, Zn²⁺, Cl⁻, I⁻, NO₃⁻) were investigated by fluorescence method. The interference resulting from 100 equivalents of these species tested individually was negligible compared to signal due to DA (Fig. S6). These results prove that the RGO-DTPA-Tb probe is selective for efficient

recognition of DA in buffer solution (PBS, pH 7.4). These data show that DA coordinates and sensitizes the terbium emissions but potential interfering substances do not.

In order to evaluate the sensitivity and selectivity of different materials modified electrodes for DA determination, the electrochemical behaviors of DA (3 μM) in the presence of AA (300 μM) were studied at the surface of bare GCE, GO/GCE, RGO-DTPA/GCE and RGO-DTPA-Tb/GCE using differential pulse voltammetry (DPV). With bare GCE (Fig. S7a), voltammetric peaks for DA and AA overlapped and had low current intensities, indicating poor selectivity and sensitivity of the unmodified electrode. A slight decrease of the peak current was observed on GO/GCE (Fig. S7b), demonstrating that GO blocks the electron transfer between DA or AA and electrode. Besides, the DA and AA peaks were not resolvable on GO/GCE. Therefore, GO is not suitable for DA detection, because it has large electronic defects on its surface that result in poor conductivity. However, RGO-DTPA/GCE exhibits two well-resolved peaks at -0.02 and 0.17 V, corresponding to the voltammetric responses of AA and DA respectively (Fig. S7c). We attribute this selectivity, firstly, to the π - π interaction between the graphene basal plane and the phenyl structure of DA molecules. Secondly, the strong electrostatic attraction between positively-charged DA and negatively-charged RGO-DTPA likely accelerates the electron transfer compared to that on the GO/GCE. Compared with RGO-DTPA/GCE, the terbium containing sample (RGO-DTPA-Tb/GCE) (Fig. S7d) had a higher voltammetric oxidation current response to DA, whereas the intensity of the oxidation peak for AA was almost unchanged. Because the incorporation of terbium ion can coordinate with DA, more dopamines are adsorbed during the oxidation reaction. The DPV response in the absence of AA is also stable (Fig. S7e), indicating that the oxidation of

DA on the RGO-DTPA-Tb/GCE was not influenced by the presence of AA. The above results demonstrate that RGO-DTPA-Tb holds promise as an electrode material for the detection of DA with high sensitivity and good selectivity.

The calibration of DA on RGO-DTPA-Tb/GCE was investigated by DPV in PBS solution (0.1 M, pH 7.4). Fig. 4 shows DPV curves of RGO-DTPA-Tb/GCE at various concentrations of DA. The peak current changed linearly with DA in the concentration range from 0.1 to 10 μM (Fig. 4, inset) and the detection limit was as low as 12 nM ($S/N = 3$). Furthermore, experiments showed that no interferences in the peak current of DA were observed in the presence of glucose, lactose, citrate, lysine, arginine, tryptophan, methionine, alanine, K^+ , Ca^{2+} , Mg^{2+} , Zn^{2+} , Cl^- , I^- , or NO_3^- . These results indicate that lanthanide complexes modified graphene hybrid materials have the potential for constructing new DA biosensors.

Conclusions

In summary, a novel graphene-based material modified with a terbium complex has been constructed to detect DA in a buffered solution. The luminescence from RGO-DTPA-Tb was greatly enhanced upon binding solely with DA. Furthermore, this hybrid material can be successfully assembled onto a glass carbon electrode, and DA was specifically detected even in the presence of large amounts of AA using DPV. Compared to a normal reduced graphene electrode,¹⁵ the RGO-DTPA-Tb/GCE offered more sensitivity and selectivity for detection of DA due to the favorable coordination and electrostatic attraction between DA and RGO-DTPA-Tb. Therefore, this novel efficient optical-electrochemical dual probe should find application in biomedical measurements.

Acknowledgments

Q. M. acknowledges the support from National Natural Science Foundation of China (No 21371063 and No 21002035). This study was supported by the Scientific Research Foundation of Graduate School of South China Normal University.

References

1. M. G. Bock and M. A. Patane, *Annu. Rep. Med. Chem.*, 2000, 35, 221-230.
2. A. Zhang, J. L. Neumeyer and R. J. Baldessarini, *Chem. Rev.*, 2007, 107, 274-302.
3. P. Damier, E. Hirsch, Y. Agid and A. Graybiel, *Brain*, 1999, 122, 1437-1448.
4. J. Smythies, *Neurotox. Res.*, 1999, 1, 27-39.
5. V. Carrera, E. Sabater, E. Vilanova and M. A. Sogorb, *J. Chromatogr. B*, 2007, 847, 88-94.
6. M. A. Fotopoulou and P. C. Ioannou, *Anal. Chim. Acta*, 2002, 462, 179-185.
7. G. H. Ragab, H. Nohta and K. Zaitso, *Anal. Chim. Acta*, 2000, 403, 155-160.
8. Y. H. Park, X. Zhang, S. S. Rubakhin and J. V. Sweedler, *Anal. Chem.*, 1999, 71, 4997-5002.
9. R. Zhu and W. T. Kok, *Anal. Chem.*, 1997, 69, 4010-4016.
10. H. Y. Wang, Y. Sun and B. Tang, *Talanta*, 2002, 57, 899-907.
11. Y. Ma, C. Yang, N. Li and X. Yang, *Talanta*, 2005, **67**, 979-983.
12. F. M. Raymo and M. A. Cejas, *Org. Lett.*, 2002, **4**, 3183-3185.
13. Y. Lin, M. Yin, F. Pu, J. Ren and X. Qu, *Small*, 2011, **7**, 1557-1561.
14. L. Wu, L. Feng, J. Ren and X. Qu, *Biosens. Bioelectron.*, 2012, **34**, 57-62.

15. Y.-R. Kim, S. Bong, Y.-J. Kang, Y. Yang, R. K. Mahajan, J. S. Kim and H. Kim, *Biosens. Bioelectron.*, 2010, **25**, 2366-2369.
16. W. Damien, *Chem. Commun.*, 2004, **6**, 732-733.
17. M. Mallesha, R. Manjunatha, C. Nethravathi, G. S. Suresh, M. Rajamathi, J. S. Melo and T. V. Venkatesha, *Bioelectrochemistry*, 2011, **81**, 104-108.
18. L. Tan, K.G. Zhou, Y.H. Zhang, H.X. Wang, X.D. Wang, Y.F. Guo and H.L. Zhang, *Electrochem. Commun.*, 2010, **12**, 557-560.
19. K. S. Novoselov, A. K. Geim, S. Morozov, D. Jiang, Y. Zhang, S. Dubonos, I. Grigorieva and A. Firsov, *Science*, 2004, **306**, 666-669.
20. X. Qi, K. Y. Pu, H. Li, X. Zhou, S. Wu, Q. L. Fan, B. Liu, F. Boey, W. Huang and H. Zhang, *Angew. Chem. Int. Ed.*, 2010, **49**, 9426-9429.
21. X. Huang, X. Qi, F. Boey and H. Zhang, *Chem. Soc. Rev.*, 2012, **41**, 666-686.
22. C. Tan, X. Huang and H. Zhang, *Mater. Today*, 2013, **16**, 29-36.
23. M. Pumera, *Chem. Soc. Rev.*, 2010, **39**, 4146-4157.
24. D. Chen, L. Tang and J. Li, *Chem. Soc. Rev.*, 2010, **39**, 3157-3180.
25. O. C. Compton, D. A. Dikin, K. W. Putz, L. C. Brinson and S. T. Nguyen, *Adv. Mater.*, 2010, **22**, 892-896.
26. C. X. Guo, H. B. Yang, Z. M. Sheng, Z. S. Lu, Q. L. Song and C. M. Li, *Angew. Chem. Int. Ed.*, 2010, **49**, 3014-3017.
27. K. Jasuja and V. Berry, *ACS nano*, 2009, **3**, 2358-2366.
28. Y. Fang and E. Wang, *Chem. Commun.*, 2013, **49**, 9526-9539.
29. Y. Shao, J. Wang, H. Wu, J. Liu, I. A. Aksay and Y. Lin, *Electroanalysis*, 2010, **22**,

1027-1036.

30. W. Ma, D. Han, S. Gan, N. Zhang, S. Liu, T. Wu, Q. Zhang, X. Dong and L. Niu, *Chem. Commun.*, 2013, **49**, 7842-7844.
31. K. Binnemans, *Chem. Rev.*, 2009, **109**, 4283-4374.
32. J.-C. G. Bunzli, *Chem. Rev.*, 2010, **110**, 2729-2755.
33. C. Tan, Q. Wang and C. Zhang, *Chem. Commun.*, 2011, **47**, 12521.
34. Z. Zhou, C. Tan, Y. Zheng and Q. Wang, *Sensor. Actuat. B-Chem.*, 2013, **188**, 1176-1182.
35. M. I. Stich, M. Schaeferling and O. S. Wolfbeis, *Adv. Mater.*, 2009, **21**, 2216-2220.
36. J. Massue, S. J. Quinn and T. Gunnlaugsson, *J. Am. Chem. Soc.*, 2008, **130**, 6900-6901.
37. S. M. Wabaidur, Z. A. Alothman and M. Naushad, *Spectrochim. Acta A*, 2012, **93**, 331-334
38. D. Lee, L. De Los Santos V, J. Seo, L. L. Felix, A. Bustamante D, J. Cole and C. Barnes, *J. Phys. Chem. B*, 2010, **114**, 5723-5728.
39. C. A. Amarnath, C. E. Hong, N. H. Kim, B.-C. Ku, T. Kuila and J. H. Lee, *Carbon*, 2011, **49**, 3497-3502.
40. J. Ho, H. Chang and W. Su, *Anal. Chem.*, 2012, **84**, 3246.

Figures Captions

Fig. 1 Schematic representation of RGO-DTPA-Tb and mechanism of luminescence enhancement by DA and the changes of its emission spectra. Differential pulse voltammetry (DPV) of RGO-DTPA-Tb assembled on electrodes with and without various concentration of DA. Photo: RGO-DTPA-Tb in PBS solution (pH 7.4) excited by UV light at 254 nm with (right) and without (left) 10 μ M of DA.

Fig. 2 SEM (a) and TEM (b) images of RGO-DTPA-Tb.

Fig. 3 Emission spectra of RGO-DTPA-Tb (1 mg/L) upon addition of 0.5-10 μ M of DA in PBS buffer solution (pH 7.4). Inset: relative intensity of RGO-DTPA-Tb at 545 nm with the concentration over a DA concentration range from 0.5-10 μ M.

Fig. 4 Differential pulse voltammetry (DPA) of RGO-DTPA-Tb assembled on a GC electrode in the presence of 0.1 to 10 μ M DA in PBS buffer solution (pH 7.4).

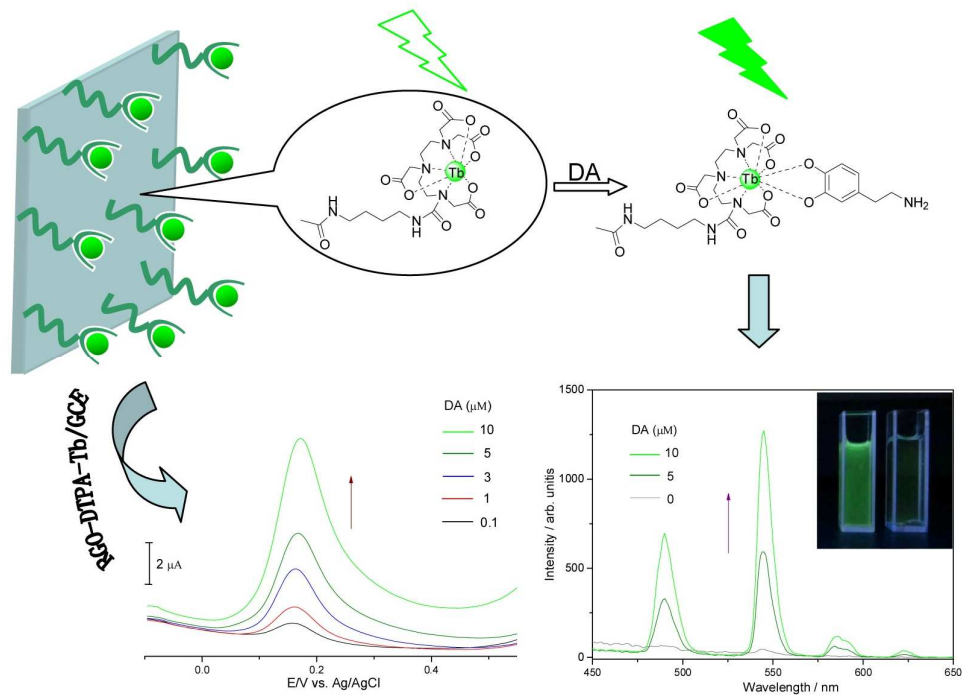
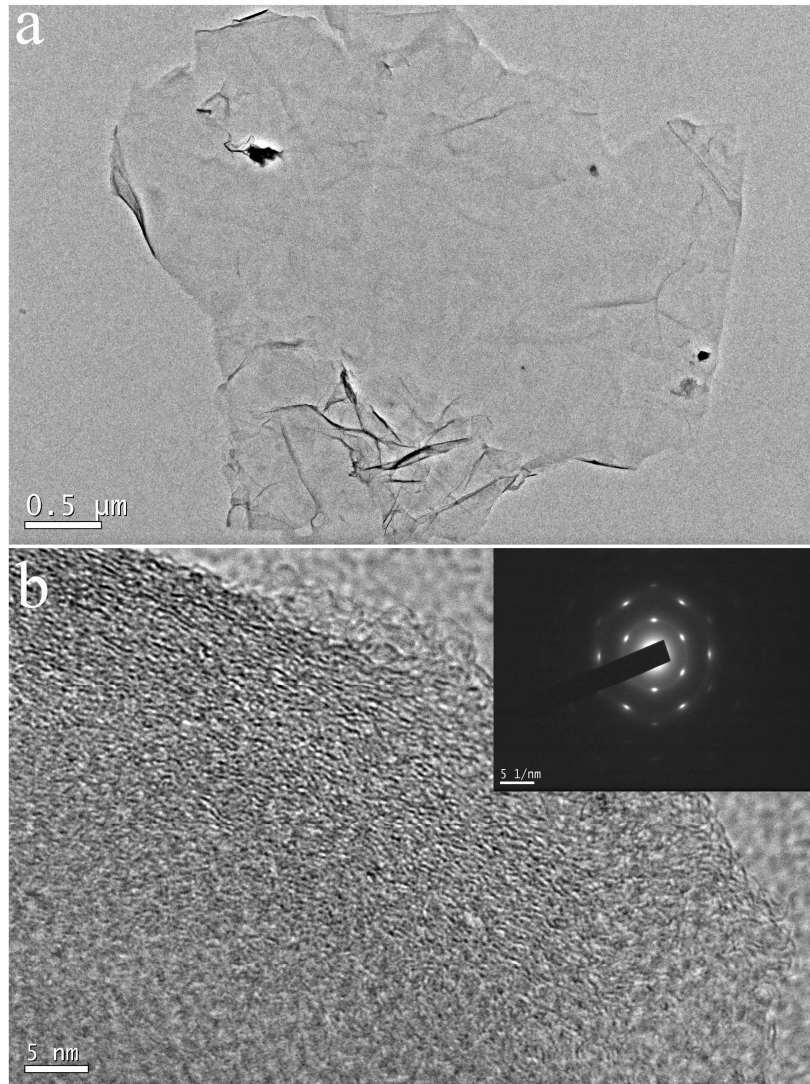


Fig. 1

**Fig. 2**

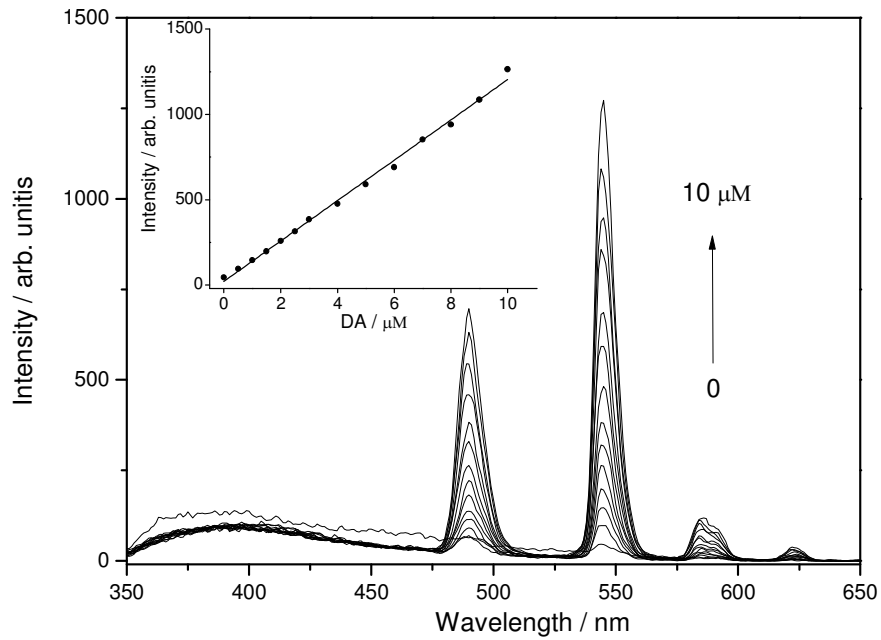


Fig. 3

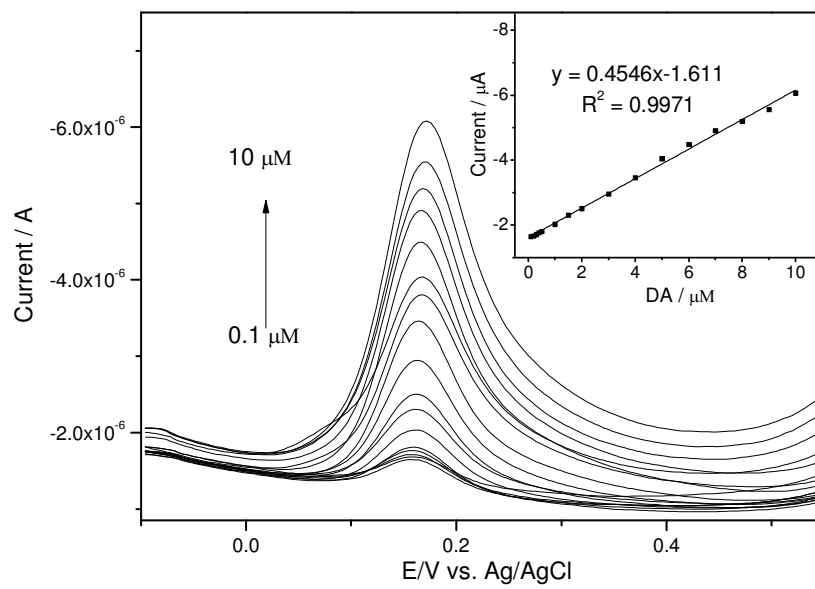


Fig. 4